Interface-driven spin-torque ferromagnetic resonance by Rashba coupling at the interface between nonmagnetic materials

M. B. Jungfleisch,[1,*] W. Zhang,[1] J. Sklenar,[1,2] W. Jiang,[1] J. E. Pearson,[1] J. B. Ketterson,[2] and A. Hoffmann[1]

[1]*Materials Science Division, Argonne National Laboratory, Argonne, Illinois 60439, USA*

[2]*Department of Physics and Astronomy, Northwestern University, Evanston, Illinois 60208, USA*

(Received 22 July 2015; revised manuscript received 30 April 2016; published 20 June 2016)

The Rashba-Edelstein effect stems from the interaction between the electron's spin and its momentum induced by spin-orbit interaction at an interface or a surface. It was shown that the inverse Rashba-Edelstein effect can be used to convert a spin current into a charge current. Here, we demonstrate the reverse process of a charge- to spin-current conversion at a Bi/Ag Rashba interface. We show that this interface-driven spin current can drive an adjacent ferromagnet to resonance. We employ a spin-torque ferromagnetic resonance excitation/detection scheme which was developed originally for a bulk spin-orbital effect, the spin Hall effect. In our experiment, the direct Rashba-Edelstein effect generates an oscillating spin current from an alternating charge current driving the magnetization precession in a neighboring permalloy (Py, $Ni_{80}Fe_{20}$) layer. Electrical detection of the magnetization dynamics is achieved by a rectification mechanism of the time dependent multilayer resistance arising from the anisotropic magnetoresistance.

DOI: 10.1103/PhysRevB.93.224419

Conventional spintronics relies on the exchange interaction between conduction electrons on one side and localized spins in magnetic materials on the other side [1]. Stimulated by the experimental demonstration of spin- to charge-current conversion using bulk spin Hall effects (SHEs), these kinds of spin-orbital phenomena were actively investigated in the last decade and opened the door to the research field of spin orbitronics [2–6]. SHEs can be investigated by means of spin-current injection from a ferromagnet (FM) into materials with large spin-orbit coupling, usually normal metals (NMs) such as Pt or Pd [7], and sensing the generated voltage generated by means of the inverse spin Hall effect (ISHE) [6,8–15]. Other interesting applications of SHEs are the effective magnetization switching of nanomagnets or the movement of domain walls [16–18]. Furthermore, the ferromagnetic linewidth modulation as well as the excitation of spin waves and ferromagnetic resonance by SHE was demonstrated in ferromagnetic metals and insulators [19–24]. The SHE is a bulk effect occurring within a certain volume of the NM determined by the spin-diffusion length. The conversion efficiency can be expressed by a material-specific parameter, the spin Hall angle γ_{SHE} [4].

Very recently, it has been shown that the inverse Rashba-Edelstein effect (IREE) can also be used for transformation of a spin current into a charge current [25–29]. The IREE is the inverse process to the Rashba-Edelstein effect (REE) [30]. The REE originates from spin-orbit interaction in a two-dimensional (2D) electron gas at interfaces or surfaces, which effectively produce a steady nonequilibrium spin polarization from a charge current driven by an electric field. The Hamiltonian of this interaction is given by [25] $H_{\mathrm{R}} = \alpha_{\mathrm{R}}(k \times \hat{e}_z) \cdot \sigma$, where α_{R} is the Rashba coefficient, $\hat{e}_z$ is the unit vector in z direction [see Figs. 1(b) and 1(c)], and σ is the vector of Pauli matrices. As a result of this interaction the dispersion curves of the 2D electron gas are spin split if $\alpha_{\mathrm{R}} \neq 0$, as illustrated in Fig. 1(a). Analogous to the spin Hall angle, the spin- to charge-current interconversion parameter can be defined as [25]

$$\lambda_{\mathrm{REE}} = \alpha_{\mathrm{R}} \tau_{\mathrm{S}} / \hbar, \tag{1}$$

where τ_{S} is the effective relaxation time describing the ratio between spin injection and spin-momentum scattering and $\hbar$ is the reduced Planck constant. The spin-split 2D electron gas dispersions and Fermi contours of many Rashba surfaces and interfaces have been investigated spectroscopically [31]. In general, large Rashba couplings occur at interfaces between heavy elements with strong spin-orbit interaction (such as Bi, Pb, and Sb) and other nonmagnetic materials with small spin-orbit coupling such as Ag, Au, and Cu [31,32]. Even though the interaction between a charge current and a nonzero spin density at a Rashba interface has been demonstrated by injection of a spin-pumping-driven spin current at ferromagnetic resonance, the reverse process remains to be explored experimentally until now.

Here, we demonstrate that a Bi/Ag Rashba interface can drive spin-torque ferromagnetic resonance (ST-FMR) in an adjacent ferromagnetic layer. We interpret our results in terms of an excitation by the direct REE, which drives an oscillating spin current from an alternating charge current that scatters at the Rashba interface (Ag/Bi). The generated spin current excites the magnetization precession in a neighboring permalloy (Py, $Ni_{80}Fe_{20}$) layer by the spin-transfer torque effect [22,33]. The precessional magnetization leads to resistance oscillations on account of the anisotropic magnetoresistance (AMR) of Py. The mixing between the applied alternating current and the oscillating resistance allows for a direct voltage detection of the induced magnetization dynamics [22,24]. Injecting an additional dc current to the sample results in an additional spin current generation due to the REE which enables one to manipulate the ferromagnetic resonance linewidth by exerting a torque on the magnetization. Besides that, we find an enhanced Gilbert damping for the trilayers and a systematic variation of the damping with the Ag interlayer thickness.

*jungfleisch@anl.gov

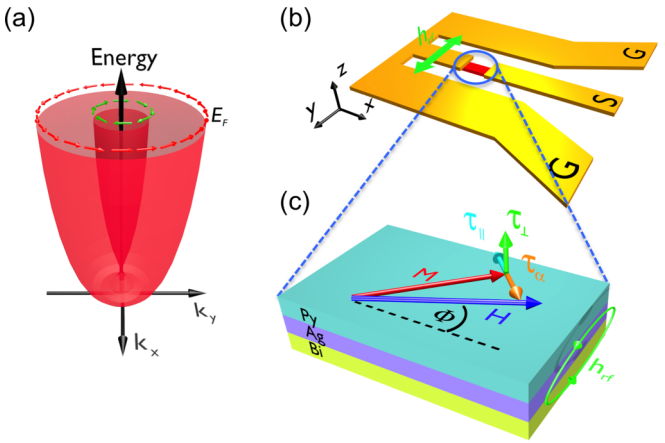

FIG. 1. (a) Dispersion curves of a 2D electron gas are spin split due to the REE. (b) Scheme of the ST-FMR experimental setup. (c) ST-FMR mechanism in Py/Ag/Bi multilayers. The alternating rf current drives an Oersted field h_{rf} exerting a fieldlike torque $\tau_\perp$ on the magnetization M. At the same time an oscillatory transverse spin accumulation at the Py/Ag interface generated at the Ag/Bi interface by the REE exerts a dampinglike torque $\tau_{||}$ on the magnetization.

We fabricated the devices using magnetron sputtering and photolithography. The multilayers were prepared in the shape of $30 \times 5\ \mu m^2$ stripes using lithography and lift-off on intrinsic Si substrates with 300-nm-thick thermally grown SiO_2. Four different types of multilayers were deposited using magnetron sputtering: Py, Py/Bi, Py/Ag, and Py/Ag/Bi. In the case of the Py/Ag/Bi systems, the Ag thickness was $t_{Ag} = 2$, 4, 6, 10, 15 nm, the Py thickness $t_{Py} = 9$ nm, and the Bi thickness $t_{Bi} = 4$ nm (resistivities $\rho_{Py} \approx 0.4\ \mu\Omega\,m$, $\rho_{Bi} \approx 4.87\ \mu\Omega\,m$, $\rho_{Ag} \approx 0.04\ \mu\Omega\,m$, [26]). The control samples feature a Py thickness of 9 nm, Ag thickness 10 nm, and Bi thickness 4 nm. In a subsequent process step, the coplanar waveguide (CPW) was fabricated on top of the multilayers. Figure 1(b) illustrates the experimental setup. A bias-T is used to apply a microwave signal and to detect the rectified dc voltage at the same time. The applied microwave power is kept constant at +10 dBm, unless otherwise mentioned. An in-plane magnetic field is applied at an angle of $\Phi = 45^\circ$ [see illustration in Figs. 1(b) and 1(c)]. While sweeping the external magnetic field the dc voltage is detected by a lock-in amplifier with an amplitude modulation of the microwave current at 3 kHz. All measurements were performed at room temperature.

Figure 2 shows typical spectra at an excitation frequency of $f = 4$ GHz. Let us first discuss the trilayers [Fig. 2(a)]. In our experiment, magnetization dynamics is excited simultaneously by the Oersted field as well as by the REE which generates an oscillating spin current from the alternating charge current driving the magnetization precession in the neighboring permalloy layer when the condition of ferromagnetic resonance is fulfilled,

$$f = \frac{|\gamma|}{2\pi}\sqrt{H(H + 4\pi M_{\text{eff}})}. \tag{2}$$

Here, M_{eff} is the effective magnetization and $|\gamma|$ is the gyromagnetic ratio. Electrical detection of the magnetization dynamics is achieved by a rectification mechanism of the time dependent multilayer resistance arising from the AMR of Py.

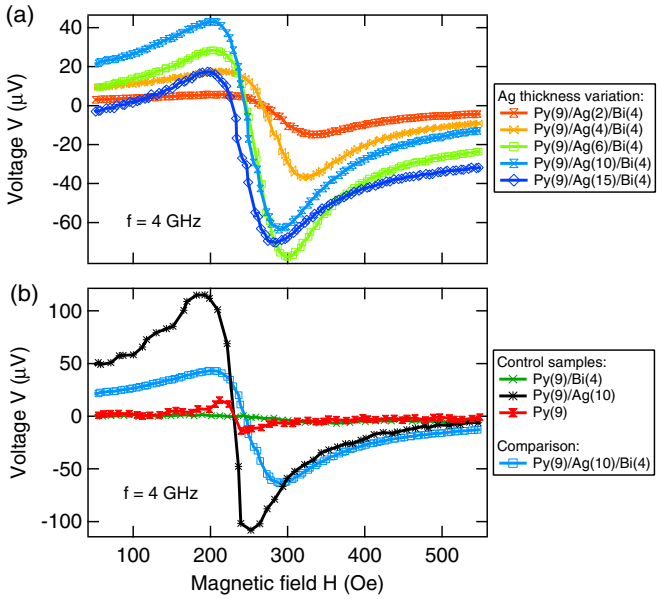

FIG. 2. Spectra of REE-driven ST-FMR measured at a frequency of 4 GHz and an applied microwave power of +10 dBm. Thickness in brackets given in nanometers. (a) Ag thickness dependence of the resonance signal. (b) Comparison between control samples and Py(9)/Ag(10)/Bi(4).

A rectification by spin pumping and IREE is a secondary effect in our experiment [see Supplemental Material (SM) [34]]. As is apparent from Fig. 2(a), the Py/Ag/Bi samples exhibit a superimposed symmetric and antisymmetric Lorentzian line shape. The smallest Ag interlayer thickness of 2 nm shows the largest symmetric contribution, but the smallest absolute signal. With increasing t_{Ag} the signal tends to be more antisymmetric and the absolute value increases. The control samples are depicted in Fig. 2(b). The pure Py sample features a small, antisymmetric Lorentzian signal due to a rectification by AMR. The Py/Bi sample exhibits a very small, mostly symmetric signal. Py/Ag features a large antisymmetric signal: The Ag layer is beneficial for the absolute voltage because a larger Oersted field is generated in the Py layer resulting in a higher AMR signal with a substantial antisymmetric line shape. We obtain the same sign in both Py/Bi and Py/Ag/Bi samples showing that the REE has the same polarity as the pure ISHE in Bi in agreement with earlier works [25,27].

The excitation of ferromagnetic resonance is confirmed by a fit to Eq. (2) [see Fig. 3(a)]. Furthermore, the data shown in Fig. 3(b) is governed by a linear dependence between linewidth ΔH and the excitation frequency f:

$$\Delta H(f) = \Delta H_0 + 4\pi f \frac{\alpha}{|\gamma|}, \tag{3}$$

where ΔH_0 is the inhomogeneous linewidth broadening given by the zero-frequency intercept and α is the Gilbert damping parameter. This confirms the excitation of FMR in our samples. As is apparent from Fig. 3(b), we observe a clear Ag-thickness dependence of the Gilbert damping parameter (slope). To highlight this observation we plotted the Gilbert damping parameter α and the inhomogeneous linewidth broadening ΔH_0 of the different samples in Fig. 3(c). The following trend

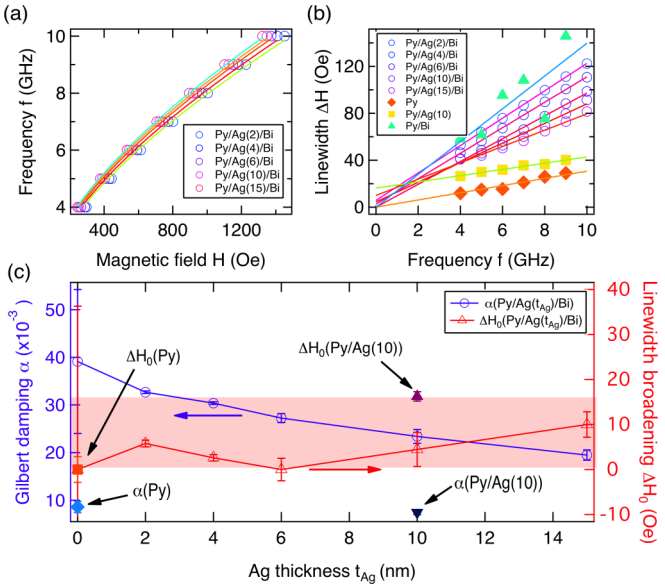

FIG. 3. (a) Frequency vs field dependence for different Ag interlayer thicknesses, $t_{Py} = 9$ nm, $t_{Bi} = 4$ nm. A fit to Eq. (2) confirms the excitation of ferromagnetic resonance (shown as solid lines). (b) Determination of Gilbert damping parameter α. Solid lines show a fit to Eq. (3). (c) Gilbert damping parameter α and inhomogeneous linewidth broadening for the different samples.

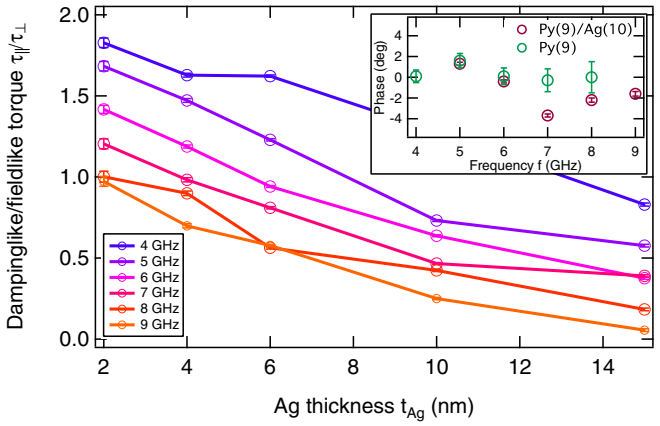

FIG. 4. Ratio dampinglike vs fieldlike torques $\tau_\parallel/\tau_\perp$ as a function of t_{Ag} for various frequencies. The inset shows the phase difference determined from the Py/Ag and Py control samples.

is observed: The Py/Bi sample ($t_{Ag} = 0$ nm) exhibits the largest α and ΔH_0, which is conceivable because Bi is known to be a good spin sink, e.g., [26,35]. Please note that the signal of the Py/Bi is very small compared to those of all other samples (see Fig. 2) and thus the error bar is larger. With increasing Ag thickness α decreases, which indicates that spin-transfer process by spin sinking/spin relaxation occurs at the Ag/Bi interface or within the first atomic layers in Bi. This process is likely due to the REE and in qualitative agreement with a three-layer spin transport model presented by Boone *et al.* [36]. The control samples Py and Py/Ag are shown for comparison, and it is found that the Gilbert damping parameter for both samples is lower than for the trilayers and the Py/Bi sample, corroborating our interpretation of an interfacial spin-transfer process at the Ag/Bi interface. An increase of ΔH_0 for the Py/Ag/Bi trilayers is observed [see Fig. 3(c)]. This is possibly due to a roughening of the Ag occurring during its growth, which then leads to a rougher Py top layer and a larger inhomogeneous linewidth.

The magnetization dynamics in a macrospin model is governed by a modified Landau-Lifshitz-Gilbert equation [24]:

$$\frac{d\hat{m}}{dt} = -|\gamma|\hat{m} \times \vec{H}_{\text{eff}} + \alpha\hat{m} \times \frac{d\hat{m}}{dt} + |\gamma|\tau_\parallel \hat{m} \times (\hat{y} \times \hat{m}) + |\gamma|\tau_\perp \hat{y} \times \hat{m}, \quad (4)$$

where $\hat{m}$ is the magnetization direction, H_{eff} is the effective magnetic field, $\tau_\parallel$ and $\tau_\perp$ are the two acting torque components, and the coordinate system $(\hat{x}, \hat{y}, \hat{z})$ is defined as shown in Figs. 1(b) and 1(c).

The two vector components of the current-induced torque $\tau_\parallel, \tau_\perp$ can be related to the line shapes of the symmetric and antisymmetric components of the resonance line shape [24]: (1) An in-plane component (dampinglike) $\tau_\parallel \sim \hat{m} \times (\hat{y} \times \hat{m})$ results in a symmetric contribution and (2) an out-of-plane component (fieldlike) $\tau_\perp \sim \hat{y} \times \hat{m}$ results in an antisymmetric contribution [see Fig. 1(c)] [24]. We employ a two-torque model capturing the two contributions $\tau_\perp$ and $\tau_\parallel$ to analyze our data (see SM). Figure 4 illustrates the Ag-thickness dependence of the ratio dampinglike vs fieldlike torques for different excitation frequencies. We find the largest ratio of the torques $\tau_\parallel/\tau_\perp$ for the smallest Ag interlayer thickness. Strikingly, this illustrates that the interfacial spin-current-driven dampinglike torque is the largest for small Ag thicknesses. With increasing Ag thickness fieldlike torques play a more important role. Furthermore, we find a frequency dependence of the torque ratio, which is usually not expected in ST-FMR. It might suggest that other effects play a role here. In order to rule out any spurious contributions that could possibly affect the line shapes, we used the Py and Py/Ag control samples to determine the phase difference between the microwave Oersted field and the alternating charge current (see SM). A nonzero phase can lead to a symmetric Lorentzian line shape which would contaminate the results. As is apparent from the inset in Fig. 4, the phase is basically zero [pure antisymmetric line shape [37]; see Fig. 2(a)] corroborating our interpretation that the observed dampinglike torque is solely due to an interfacial REE rather than due to other spurious effects such as AMR of Py. In order to gain further insights into the involved effects, in-plane angular dependent measurements were performed. The symmetric and antisymmetric components to the signal follow a $\cos(\phi)\sin(2\phi)$ corroborating the two-torque model (see SM). Conventional angular dependent magnetoresistance measurements reveal a value of $dR/d\phi$ of the order of a few Ω/rad (SM).

According to the spin-torque theory [33], an additional spin current injected into the FM layer will increase or decrease the effective magnetic damping, i.e., the linewidth, depending on its relative orientation with respect to the magnetization [22,23]. Since Ag features a very small spin Hall angle [39] and our Bi layer is almost nonconducting [26], the demonstration of the ferromagnetic linewidth manipulation by an additional dc current injection would be an independent manifestation of

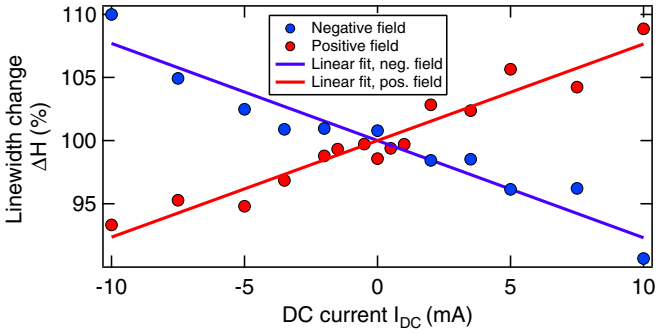

FIG. 5. Manipulation of the FMR linewidth by a simultaneous injection of an electrical dc current. The zero-current linewidth is 27.5 Oe. Py(15)/Ag(4)/Bi(4), $f = 4$ GHz, $P_{RF} = +2$ dBm. Comparative control measurements on Py(15)/Ag(4) did not show any dc linewidth modulation, not shown here.

charge- to spin-current conversion by the REE. Figure 5 shows unambiguously that it is indeed possible to manipulate the resonance line shape if an additional dc current is injected into the sample. For this purpose a rather small rf power of +2 dBm is chosen. Apparently, for a positive magnetic field polarity, a positive dc current leads to an enhanced linewidth, i.e., a damping enhancement. In contrast, a negative current leads to a decreased linewidth, i.e., a damping reduction. Reversing the field polarity results in an opposite trend. It might be possible to improve the efficiency of the observed effects by using epitaxially grown samples. In fact, it is known from first-principle calculations that a (111) orientation yields a large Rashba spin splitting [40,41] and thus, presumably a larger interface-driven ST-FMR.

Although it is not physical to speak of a thickness in the case of an interface effect, it is still possible to adapt a line shape analysis approach which was presented originally in Ref. [22] to relate the spin Hall angle to the ratio symmetric/antisymmetric components of the resonance line shape. We can estimate a spin Hall angle equivalent γ^* if we hypothetically assume that the charge-spin conversion process was a bulk-driven rather than an interface-driven effect [22]:

$$\gamma^* = \frac{S}{A}\frac{e\mu_0 M_S t_{Py} t_{NM}}{\hbar}\sqrt{1+\frac{4\pi M_{eff}}{H}}. \quad (5)$$

Here, t_{NM} is the nonmagnetic layer thickness. We find the spin Hall angle equivalent to be $\gamma^* \approx 18\%$ for our Py/Ag/Bi samples (average value for different Ag thicknesses), exceeding most paramagnetic metals. In our previous work we determined the REE conversion parameter $\lambda_{REE} \approx 0.1$ nm [26]. Using the relation $\lambda_{REE} = 1/2d\gamma^*$, where d is the *interface layer* thickness [25], we obtain $d \approx 1$ nm, which is a reasonable estimate. Finally, we note that the resistivities of our materials are larger than for thicker films, which might indicate an enhanced interface scattering. Thus, the observed effect might have contributions from electron scattering in the Bi layer partially leading to a spin-current generation at the Bi surface by the spin-Hall effect.

In summary, we demonstrated the conversion of a charge current into a spin current by Rashba coupling of interface states by adapting a spin-torque ferromagnetic resonance excitation/detection technique. The Ag thickness dependence clearly demonstrates that the spin dynamics in the adjacent Py layer is driven by an interface-generated spin-polarized electron current that exerts a torque on the magnetization rather than a bulk effect such as the spin Hall effect. Our conclusions are further validated by a FMR linewidth modulation due to the spin current injection by applying an additional dc charge current to the sample stack. Our results will stimulate experimental and theoretical endeavors to explore novel interface- and surface-driven spin-orbital phenomena for the efficient excitation of magnetization dynamics.

We thank Roland Winkler for illuminating discussions. This work was supported by the U.S. Department of Energy, Office of Science, Materials Science and Engineering Division. Lithography was carried out at the Center for Nanoscale Materials, an Office of Science user facility, which is supported by DOE, Office of Science, Basic Energy Science under Contract No. DE-AC02-06CH11357.

[1] I. Žutić, J. Fabian, and S. Das Sarma, Rev. Mod. Phys. **76**, 323 (2004).
[2] M. I. D'yakonov and V. I. Perel', JETP Lett. **13**, 467 (1971).
[3] J. E. Hirsch, Phys. Rev. Lett. **83**, 1834 (1999).
[4] A. Hoffmann, IEEE Trans. Magn. **49**, 5172 (2013).
[5] Y. Kajiwara, K. Harii, S. Takahashi, J. Ohe, K. Uchida, M. Mizuguchi, H. Umezawa, H. Kawai, K. Ando, K. Takanashi, S. Maekawa, and E. Saitoh, Nature (London) **464**, 262 (2010).
[6] M. B. Jungfleisch, W. Zhang, W. Jiang, and A. Hoffmann, SPIN **05**, 1530005 (2015).
[7] W. Zhang, M. B. Jungfleisch, W. Jiang, Y. Liu, J. E. Pearson, S. G. E. te Velthuis, A. Hoffmann, F. Freimuth, and Y. Mokrousov, Phys. Rev. B **91**, 115316 (2015).
[8] O. Mosendz, J. E. Pearson, F. Y. Fradin, G. E. W. Bauer, S. D. Bader, and A. Hoffmann, Phys. Rev. Lett. **104**, 046601 (2010).
[9] O. Mosendz, V. Vlaminck, J. E. Pearson, F. Y. Fradin, G. E. W. Bauer, S. D. Bader, and A. Hoffmann, Phys. Rev. B **82**, 214403 (2010).
[10] W. Zhang, M. B. Jungfleisch, W. Jiang, J. E. Pearson, A. Hoffmann, F. Freimuth, and Y. Mokrousov, Phys. Rev. Lett. **113**, 196602 (2014).
[11] E. Saitoh, M. Ueda, H. Miyajima, and G. Tatara, Appl. Phys. Lett. **88**, 182509 (2006).
[12] A. Azevedo, L. H. Vilela Leão, R. L. Rodriguez-Suarez, A. B. Oliveira, and S. M. Rezende, J. Appl. Phys. **97**, 10C715 (2005).
[13] W. Zhang, M. B. Jungfleisch, W. Jiang, J. Sklenar, F. Y. Fradin, J. E. Pearson, J. B. Ketterson, and A. Hoffmann, J. Appl. Phys. **117**, 172610 (2015).

[14] M. B. Jungfleisch, A. V. Chumak, V. I. Vasyuchka, A. A. Serga, B. Obry, H. Schultheiss, P. A. Beck, A. D. Karenowska, E. Saitoh, and B. Hillebrands, Appl. Phys. Lett. **99**, 182512 (2011).

[15] M. B. Jungfleisch, A. V. Chumak, A. Kehlberger, V. Lauer, D. H. Kim, M. C. Onbasli, C. A. Ross, M. Kläui, and B. Hillebrands, Phys. Rev. B **91**, 134407 (2015).

[16] D. C. Ralph and M. D. Stiles, J. Magn. Magn. Mater. **320**, 1190 (2008).

[17] A. Hoffmann and H. Schultheiß, Curr. Opin. Solid State Mater. Sci. **19**, 253 (2014).

[18] W. Jiang, P. Upadhyaya, W. Zhang, G. Yu, M. B. Jungfleisch, F. Y. Fradin, J. E. Pearson, Y. Tserkovnyak, K. L. Wang, O. Heinonen, S. G. E. te Velthuis, and A. Hoffmann, Science **349**, 283 (2015).

[19] A. Hamadeh, O. d'Allivy Kelly, C. Hahn, H. Meley, R. Bernard, A. H. Molpeceres, V. V. Naletov, M. Viret, A. Anane, V. Cros, S. O. Demokritov, J. L. Prieto, M. Muñoz, G. de Loubens, and O. Klein, Phys. Rev. Lett. **113**, 197203 (2014).

[20] J. Sklenar, W. Zhang, M. B. Jungfleisch, W. Jiang, H. Chang, J. E. Pearson, M. Wu, J. B. Ketterson, and A. Hoffmann, Phys. Rev. B **92**, 174406 (2015).

[21] M. B. Jungfleisch, W. Zhang, J. Sklenar, J. Ding, W. Jiang, H. Chang, F. Y. Fradin, J. E. Pearson, J. B. Ketterson, V. Novosad, M. Wu, and A. Hoffmann, Phys. Rev. Lett. **116**, 057601 (2016).

[22] L. Liu, T. Moriyama, D. C. Ralph, and R. A. Buhrman, Phys. Rev. Lett. **106**, 036601 (2011).

[23] Z. Wang, Y. Sun, M. Wu, V. Tiberkevich, and A. Slavin, Phys. Rev. Lett. **107**, 146602 (2011).

[24] A. R. Mellnik, J. S. Lee, A. Richardella, J. L. Grab, P. J. Mintun, M. H. Fischer, A. Vaezi, A. Manchon, E.-A. Kim, N. Samarth, and D. C. Ralph, Nature (London) **511**, 449 (2014).

[25] J. C. Rojas Sánchez, L. Vila, G. Desfonds, S. Gambarelli, J. P. Attané, J. M. De Teresa, C. Magén, and A. Fert, Nat. Commun. **4**, 2944 (2013).

[26] W. Zhang, M. B. Jungfleisch, W. Jiang, J. E. Pearson, and A. Hoffmann, J. Appl. Phys. **117**, 17C727 (2015).

[27] S. Sangiao, J. M. De Teresa, L. Morellon, I. Lucas, M. C. Martinez-Velarte, and M. Viret, Appl. Phys. Lett. **106**, 172403 (2015).

[28] A. Nomura, T. Tashiro, H. Nakayama, and K. Ando, Appl. Phys. Lett. **106**, 212403 (2015).

[29] M. Isasa, M. C. Martínez-Velarte, E. Villamor, C. Magén, L. Morellón, J. M. De Teresa, M. R. Ibarra, G. Vignale, E. V. Chulkov, E. E. Krasovskii, L. E. Hueso, and F. Casanova, Phys. Rev. B **93**, 014420 (2016).

[30] V. M. Edelstein, Solid State Commun. **73**, 233 (1990).

[31] C. R. Ast, J. Henk, A. Ernst, L. Moreschini, M. C. Falub, D. Pacilé, P. Bruno, K. Kern, and M. Grioni, Phys. Rev. Lett. **98**, 186807 (2007).

[32] Y. M. Koroteev, G. Bihlmayer, J. E. Gayone, E. V. Chulkov, S. Blügel, P. M. Echenique, and Ph. Hofmann, Phys. Rev. Lett. **93**, 046403 (2004).

[33] J. C. Slonczewski, J. Magn. Magn. Mater. **159**, L1 (1996).

[34] See Supplemental Material at http://link.aps.org/supplemental/10.1103/PhysRevB.93.224419 for details on the analysis and angular-dependent data.

[35] D. Hou, Z. Qiu, K. Harii, Y. Kajiwara, K. Uchida, Y. Fujikawa, H. Nakayama, T. Yoshino, T. An, K. Ando, X. Jin, and E. Saitoh, Appl. Phys. Lett. **101**, 042403 (2012).

[36] C. T. Boone, H. T. Nembach, J. M. Shaw, and T. J. Silva, J. Appl. Phys. **113**, 153906 (2013).

[37] If the Py/Ag data was affected by spin Hall effects, we would observe a substantial symmetric contribution to line shape. However, this is not the case. Since Ag features a long spin-diffusion length of $\sim$300 nm [38], it would also be possible that the spin Hall effect in Bi generates a spin current which diffuses through the Ag layer. However, since the generated voltage for the control sample Py/Bi is negligibly small [see Fig. 2(b)], this mechanism can also be ruled out.

[38] Y. Fukuma, L. Wang, H. Idzuchi, S. Takahashi, S. Maekawa, and Y. Otani, Nat. Mater. **10**, 527 (2011).

[39] H. L. Wang, C. H. Du, Y. Pu, R. Adur, P. C. Hammel, and F. Y. Yang, Phys. Rev. Lett. **112**, 197201 (2014).

[40] G. Bian, X. Wang, T. Miller, and T.-C. Chiang, Phys. Rev. B **88**, 085427 (2013).

[41] L. Moreschini, A. Bendounan, I. Gierz, C. R. Ast, H. Mirhosseini, H. Höchst, K. Kern, J. Henk, A. Ernst, S. Ostanin, F. Reinert, and M. Grioni, Phys. Rev. B **79**, 075424 (2009).